Shot noise in charge and magnetization currents of a quantum ring.

Fabio Cavaliere[1,2], Federica Haupt[2], Rosario Fazio[3], and Maura Sassetti[2]

[1] *I. Institut für Theoretische Physik, Universität Hamburg, Jungiusstraße 9, 20355 Hamburg, Germany*

[2] *LAMIA-INFM and Dipartimento di Fisica, Via Dodecaneso 33, 16146 Genova, Italy*

[3] *NEST-INFM and Scuola Normale Superiore, Piazza dei Cavalieri 7, I-56126 Pisa, Italy*

(Dated: December 10, 2004)

The shot noise in a quantum ring, connected to leads, is studied in the presence of electron interactions in the sequential tunneling regime. Two qualitatively different noise correlations with distinctly different behaviors are identified and studied in a large range of parameters. Noise in the total current is due to the discreteness of the electron charge and can become super-Poissonian as result of electron interaction. The noise in the magnetization current is comparatively insensitive to the interaction but can be greatly enhanced if population inversion of the angular states is assumed. The characteristic time scales are studied by a Monte-Carlo simulation.

PACS numbers: 73.50.Td,71.10.Pm,73.23.-b

Noise is known to be a key tool to study non-equilibrium transport properties of mesoscopic quantum systems [1]. In the regime of Coulomb Blockade the presence of electron interaction generally leads to a *suppression* of the noise as compared with the Poissonian limit [2]. Recently, several mechanisms have been proposed leading to an *enhancement* of the shot noise. A super-Poissonian regime has been found in the presence of a negative differential conductance [3], for resonant tunneling [4] and via localized states [5]. Super-Poissonian noise is also expected in a few-level quantum dot in the presence of a magnetic field [6].

In this work, we study current correlations in a one-dimensional (1D) quantum ring, connected via tunnel contacts to external leads, in the presence of interactions. The system is characterized by discrete charge and angular momentum degrees of freedom, and can be used to study interaction-induced noise effects of an unprecedented richness, in the presence of an Aharonov-Bohm flux threading the ring. We characterize the noise by considering both the *charge current noise* (related to the fluctuations of the tunneling current) and the *magnetization current noise* (related to the fluctuations in the persistent current). Our main results are: (i) regions of super-Poissonian charge noise can be found whenever high orbital channels contribute to transport. (ii) Charge noise is sensitive to asymmetry of the tunnel barriers; by changing the Aharonov-Bohm flux the charge noise can be tuned from sub- to super-Poissonian. (iii) The magnetization noise is considerably stable against asymmetry and the presence of interactions. In order to enter a regime of high magnetization noise, it is necessary to have *population inversion* in the orbital states.

All of the phenomena discussed below *cannot* be observed in a non-interacting system and should be accessible with presently available experimental technology.

For the isolated quantum ring we assume a spinless Luttinger liquid (LL) with density-density electron interactions (g interaction parameter, $g = 1$ no interaction) [7]

$$H_{\rm ring} = \frac{E_N}{2}(N - N_{\rm g})^2 + \frac{E_J}{2}\left(J - 2\frac{\Phi}{\Phi_0}\right)^2 + \sum_{n>0} n\varepsilon\, b_n^\dagger b_n\,. \tag{1}$$

The zero mode $N = N_+ + N_-$ represents the total number excess of electrons, $J = N_+ - N_-$ gives the imbalance between clockwise (N_+) and anticlockwise (N_-) moving electrons and N, J have integer eigenvalues with selection rules $(-1)^N = (-1)^J$ [8]. The gate charge is $N_{\rm g}$ and the flux is Φ, with $\Phi_0 = h/e$ the flux quantum. The charging energy E_N is mainly due to the Coulomb interaction and influenced by the coupling with the external circuit. It is the largest energy scale in the model. The orbital addition energy is $E_J = \pi v_{\rm F}/L \ll E_N$ ($v_{\rm F}$ Fermi velocity, L circumference of the ring). The last term in Eq.(1) represents plasmons moving with a renormalized velocity $v = v_{\rm F}/g$ and excitation energy $\varepsilon = 2\pi v/L$.

The ring is connected to external leads via tunneling barriers. This creates charge, $I_N^{(i)}$, and orbital, $I_J^{(i)}$, tunnel currents related to the clockwise and anticlockwise contributions: $I_N^{(i)} = I_+^{(i)} + I_-^{(i)}$ and $I_J^{(i)} = I_+^{(i)} - I_-^{(i)}$ at junctions ($i = 1, 2$). The tunneling processes modify charge and magnetization via $\dot{N} \propto I_N$ and $\dot{J} \propto I_J$.

We evaluate the zero frequency correlators ($\nu = N, J$)

$$S_\nu^{(ij)} = \int_{-\infty}^{\infty} \mathrm{dt}\ \langle \Delta I_\nu^{(i)}(t)\Delta I_\nu^{(j)}(0) + \Delta I_\nu^{(i)}(0)\Delta I_\nu^{(j)}(t)\rangle \tag{2}$$

at terminals i and j, between current fluctuations $\Delta I_\nu^{(i)}(t) = I_\nu^{(i)}(t) - \langle I_\nu^{(i)}\rangle$. The knowledge of S_N and S_J are ingredients for determining the auto- (S_{++}, S_{--}) and cross-correlators (S_{+-}, S_{-+}).

The leads are assumed as interacting LLs with interaction parameter g_ℓ. They can be realized as edge states of fractional quantum Hall liquids [9] or in quantum wires [10]. The difference of their chemical potential is controlled by the external bias voltage $\mu_2 - \mu_1 = eV$.

For weak coupling (level broadening due to tunneling much smaller than temperature and level spacing) the electronic states $|\alpha\rangle$ are occupied with probability $P_\alpha(t)$. We assume fast plasmon relaxation (see Ref.[11] for the opposite situation) towards thermal equilibrium, and we consider $k_\mathrm{B}T, eV \ll E_N$ so that the transport is governed just by two charge states N and $N+1$. The ring states are then completely characterized by their angular degree of freedom J. From now on, the index N is omitted. In the non-linear regime ($eV > E_J$) many orbital states $J_\mathrm{min} \le J \le J_\mathrm{max}$ contribute to transport. For $\Phi = 0$, $J_\mathrm{max} = -J_\mathrm{min}$. Schemes of the relevant transport states are shown in Fig. 1.

The vector $\mathbf{P} \equiv \{P_{J_\mathrm{min}}, \ldots, P_{J_\mathrm{max}}\}$ represents the occupation probabilities. It is governed by the master equation $\dot{\mathbf{P}}(t) = M \cdot \mathbf{P}(t)$. The square matrix M contains the tunneling rates $\gamma^{(i)}_{J\to J'}$ [12] through the i-th barrier with $J' = J \pm 1$. Following [2], we calculate the correlation functions $S_\nu^{(ij)}$ by spectrally decomposing M. Because of charge conservation $\langle I_\nu^{(i)}\rangle = \langle I_\nu\rangle$, and $S_\nu^{(ij)} = S_\nu$ independently of the barrier indices.

We first consider $\Phi = 0$ and voltages that allow $J_\mathrm{max} = 2$ (Fig. 1a). We consider the charge current Fano factor $F_N = S_N/2e|\langle I_N\rangle|$ and define an angular current Fano factor $F_J = S_J/2e|\langle I_N\rangle|$ related to fluctuations of I_J. We quote, for the discussion, the zero temperature case which, however, describes very accurately the temperature regime $k_\mathrm{B}T < 0.1E_J$

$$F_N = 1 + 2\,\frac{r_1(1-r_2)^2 - (1+r_1r_2)(1+r_1)\tau_1/\tau_0}{\left[1 + r_1r_2 + (1+r_1)\tau_1/\tau_0\right]^2} \tag{3}$$

$$F_J = 1 - 2r_1(1-r_1)/(1+r_1) \tag{4}$$

$$r_1 = \gamma^{(1)}_{1\to2}/\gamma^{(1)}_{1\to0}\,, \quad r_2 = 2\gamma^{(2)}_{0\to1}/\gamma^{(2)}_{2\to1} = \tau_2/\tau_0\,. \tag{5}$$

Here, r_2 represents the escape ratio from $J = 0$ and $|J| = 2$, r_1 is the population ratio between $|J| = 2$ and $J = 0$, and $r_1 \cdot r_2$ is the stationary occupation probability ratio $2P_2/P_0$. The corresponding dwell times $\tau_{|J|}$ are: $\tau_0^{-1} = 2\gamma^{(2)}_{0\to1}$, $\tau_1^{-1} = \gamma^{(1)}_{1\to2} + \gamma^{(1)}_{1\to0}$ and $\tau_2^{-1} = \gamma^{(2)}_{2\to1}$. For $J_\mathrm{max} = 1$ (Fig. 1a yellow), $r_1 = 0$ and the above expressions reduce to the results for a three channel system, $F_N < 1$, and $F_J = 1$ [2, 13, 14], which implies $F_{+-} \propto F_N - F_J < 0$. For $J_\mathrm{max} = 2$ (Fig. 1a cyan), $r_1 \neq 0$ and a new dynamics is found. Here, when the degeneracy of the dwell times τ_0 and τ_2 is lifted, $r_2 \neq 1$, the charge noise becomes super-Poissonian, $F_N > 1$, for asymmetries of the two barriers larger than

$$A_\mathrm{c} = \frac{2\bar\gamma^{(2)}_{0\to1}}{\bar\gamma^{(1)}_{1\to0} + \bar\gamma^{(1)}_{1\to2}}\,\frac{(1+r_1r_2)(1+r_1)}{r_1(1-r_2)^2} \tag{6}$$

(the asymmetry A is defined as the ratio of the high temperature tunneling resistances of the two barriers). The $\bar\gamma$ rates are defined modulo the latter resistances. The angular Fano factor F_J depends *only* on r_1 and $F_J > 1$ can be achieved when $r_1 > 1$, i.e. with a *population inversion* between transitions $1 \to 2$ and $1 \to 0$ (cf. Eq. (5)).

For interaction $0.5 < g < 1$, the region with $J_\mathrm{max} = 2$ is split by the line $E_{2\to1} = eV/2 + E_N(N_\mathrm{g} - 1/2) + 3E_J/2 = \varepsilon$ (green line in Fig. 1a), corresponding to the transition $2 \to 1$ with a plasmonic excitation in the final state. We denote these regions as I and II, depending on $E_{2\to1} < \varepsilon$ or $> \varepsilon$. If $g = 1$, only region II is present, if $g < 0.5$, there is only region I.

Figure 2 shows charge and magnetization Fano factors along the dashed-dotted red line in Fig. 1a, i.e. as a function of $(eV - 2.43E_J)/\varepsilon$, where V varies according to $N_\mathrm{g} = 1/2 + 0.93E_J/E_N - eV/2E_N$. Without interaction (magenta) the degeneracy of the plasmon energy, $\varepsilon = 2E_J$, implies $r_2 = 1$ and $r_1 < 1$, leading *always* to sub-Poissonian noise. With interaction one has $r_2 \neq 1$ so that $F_N > 1$ if $A > A_\mathrm{c}$. This result is robust against changes of strength and sign of the interaction. For F_J, the sign of the interaction is crucial. Only for attractive leads, $g_\ell > 1$, it is possible to achieve an inversion of population with $F_J > 1$ (Fig. 2b blue).

In region I, for $g < 1$ and $g_\ell = 1$, it is always $r_2 = 2$ and one can identify two energy intervals, $\sigma_\pm(n)$, corresponding to different population regions: $r_1 = 1$ in $\sigma_-(n)$ and $r_1 = n/(n+1)$ in $\sigma_+(n)$. Referring to Fig. 2, $\sigma_-(n)$ is given by $(n-1)\varepsilon < eV - 2.43E_J < (n-g)\varepsilon$ and $\sigma_+(n)$ by $(n-g)\varepsilon < eV - 2.43E_J < n\varepsilon$. In the first interval, for $A \gg A_c$ the system belongs to a universality class with values $F_N = 1 + 2/9$ and $F_J = 1$. By tuning the voltage along the diagonal line one enters periodically the interval $\sigma_+(n)$ where the Fano factors depend on the interaction, $\lambda = (g + g^{-1})/2$

$$F_N = 1 + \frac{2n(n+\lambda)}{(3n+\lambda)^2}\,, \quad F_J = 1 - \frac{2n\lambda}{(n+\lambda)(2n+\lambda)}\,. \tag{7}$$

Interactions in the leads ($g_\ell \neq 1$) modify the above modulation introducing a power law behavior at the thresholds of each region. For strong repulsive interaction, $g_\ell < 0.5$, the memory of plasmons is completely lost, with an increase of F_N and a depletion of F_J (green curves).

In Fig. 3, the critical asymmetry A_c is plotted in the plane XY, where $X = 1/2 - N_g - 1.5E_J/E_N + eV/2E_N$ and $Y = -1/2 - N_g - 0.5E_J/E_N + eV/2E_N$. Note that $Y = 0$ corresponds to the transition line $0 \to 1$, $Y = 0.03$ to the line $E_{2\to1} = \varepsilon$, and $X = 0$ to the line $1 \to 2$ (cf. Fig. 1a). In the panels a and b, the regions I and II are shown.

In both regions, near certain lines parallel to the X axis, we have $r_2 = 1$. Here, A_c diverges and no super-Poissonian charge noise can be achieved. Away from these lines, increasing the voltage, A_c decreases because of the *increasing number of excited plasmons* present in the output transition. These randomize the system and decrease the dwell time τ_1 renormalizing the output barrier having even $A_c < 1$ for sufficiently high voltage.

For $\Phi \neq 0$, the degeneracy of the states with $\pm J$ is lifted. As a consequence, each transition line at $\Phi = 0$ splits in two, which move in opposite directions when increasing Φ (Fig. 1b). This causes several effects in transport regions where $J_{\max} \neq -J_{\min}$.

Figure 4 shows results for F_N and F_J along a diagonal line (inside region II at $\Phi = 0$) for $0 < \Phi < \Phi_0/2$. Results for $\Phi_0/2 < \Phi < \Phi_0$ are specular with respect to the $\Phi = \Phi_0/2$ axis and periodic in the flux with period $\Phi = \Phi_0$. Increasing Φ, many transitions cross the fixed line, so that one can study the correlations in a wide range of transport regions. As shown in Fig. 4a, the noise can change dramatically by tuning the flux. At $\Phi = 0$ one has $A < A_c$, so that $F_N < 1$. However, increasing the flux at fixed energy, super-Poissonian noise is reached for $\Phi \approx 0.4\Phi_0$. The onset of this region is at $\Phi^* = 0.35\Phi_0$, given by the intersection of the line along where V is varied, $N_g = 1/2 + 1.7E_J/E_N - eV/2E_N$, with the upper moving transition line $2 \to 1$ with one plasmon, $N_g = 1/2 + E_J/2E_N(4/g - 3 + 4\Phi/\Phi_0) - eV/2E_N$, i.e. $\Phi^* = [1.7 + (3 - 4/g)/2]\Phi_0/2$. Inducing transitions between sub- and super-Poissonian behavior as a function of the flux is strictly a signature of interactions. In a noninteracting ring we *always* find sub-Poissonian behavior, regardless of the number of states supporting the transport. For the magnetization current, the interaction in the ring and finite flux are not enough to induce $F_J > 1$ (Fig. 4b). The flux allows to control systematically the sign of cross-correlators $F_{+-} \propto F_N - F_J$ by varying Φ. For instance $F_{+-} < 0$ for $E, \Phi \approx 0$. For $\Phi \approx 0.4\Phi_0$, where F_N is super-Poissonian and F_J has a minimum, $F_{+-} > 0$.

We conclude by presenting an interpretation of the influence of the time scales on the correlations. For this purpose, we have done a Monte-Carlo simulation [15]. The time evolution of the system making transitions with fixed conditional probability is followed. A transition $J \to J'$ occurs with probability $\gamma_{J\to J'} / \sum_{J''=J\pm1} \gamma_{J\to J''}$ ($-2 \leq J, J', J'' \leq 2$, $|J - J'| = 1$). We consider $A \gg A_c$ and $\Phi = 0$.

Figure 5 shows results of the simulation of tunneling events (black and white dots) at junction 2. Colored bars describe the sequences of J values: green bars denote $J = 0$, and red bars the excited state with $J = 2$. We denote these two sequences as S_0 and S_2. The average time interval between tunneling is τ_0 in S_0 and τ_2 in S_2 with corresponding average number of transitions $n_0 = (1 + r_1)/r_1$ and $n_2 = (1 + r_1)$ respectively. Only without interactions (Fig. 5a) the tunneling events are uniformly distributed ($\tau_0 = \tau_2$). The super-Poissonian character of F_N is due to inhomogeneous distribution of the time scales ($\tau_0 \neq \tau_2$), with bunches of events separated by longer times. The bunching tendency can be present inside S_0 (Fig. 5b, d) or inside S_2 (Fig. 5c). In all cases $F_N > 1$ independent of whether S_0 or S_2 are responsible for the bunching. However, bunching alone is not sufficient for $F_N > 1$; if $A < A_c$ bunching might still occur but the interplay of the two barriers gives $F_N < 1$. The interpretation of F_J is distinctly different. Here, the time scales $\tau_{0,2}$ do not play any role. The important parameter is the number of event n_2 in which the ring is in the excited state $J = 2$. The condition $F_J > 1$ is fulfilled only for $n_2 > 2$, *independent of bunching* (Fig. 5d).

The simulations allow also an estimate of the correlations times for the charge current, T_N, and magnetization current, T_J, which determine the relaxation dynamics for long times. This, at first glance, is only a qualitative description, which however, can be confirmed by evaluation of the time-dependent solutions of the master equation. The sequences S_0 and S_2 have average duration times $T_0 = n_0\tau_0$ and $T_2 = n_2\tau_2$. From Fig. 5b-d, one concludes that for the relaxation time of the angular momentum only the S_2 sequences contribute (red). Here $|J| = 2$ before

a transition to $J = 0$, such that $T_J = T_2$. On the other hand, the charge correlation time is determined by the two sequences and is dominated by smallest of T_0 and T_2 since $T_{\rm N}^{-1} \equiv T_0^{-1} + T_2^{-1}$.

In summary, we have investigated zero frequency shot noise of a 1D quantum ring attached to semi-infinite leads in the sequential tunneling regime. In addition to the usual charge current noise we have identified a magnetization current shot noise which characterizes the fluctuations in the angular current in the ring and has distinctly different properties. For the charge current noise a Fano factor larger than 1 indicates bunching and super-Poissonian statistics. This is closely related to the presence of interaction between the electrons in the ring and in the leads. For the magnetization current noise it is very difficult to achieve a Fano factor larger than one. It is independent of whether or not bunching occurs and is closely related to the occupation dynamics of angular states with $J > 1$. In our example, a magnetization noise Fano factor larger than 1 can only be reached when population inversion is achieved and this is done by attractive interactions in the leads. In order to verify the predicted effect experimentally, one needs to separate from the total noise the magnetization current contribution. This might be done by measuring the magnetization [16] of a single wall nanotube ring [17] or semiconductor ring [18] attached to leads.

We thank Bernhard Kramer for useful discussions and acknowledge financial support from EU-RTN HPRN CT 2000-00144, PRIN-2002 and Firb.

[1] Ya.M. Blanter, and M. Büttiker, Phys. Rep. **336**, 1 (2000).
[2] S. Hershfield, J. H. Davies, P. Hyldgaard, C. J. Stanton, and J. W. Wilkins, Phys. Rev. B **47**, 1967 (1993); A.N. Korotkov, Phys. Rev. B **49**, 10381 (1994).
[3] G. Kießlich, A. Wacker, and E. Schöll, Phys. Rev. B **68**, 125320 (2003); A. Thielmann *et al.*, cond-mat/0406647.
[4] A. Nauen, F. Hohls, J. Konemann, and R. J. Haug, Phys. Rev. B **69**, 113316 (2004).
[5] S.S. Safonov *et al.*, Phys. Rev. Lett. **91**, 136801 (2003).
[6] A. Cottet, W. Belzig, and C. Bruder, Phys. Rev. B **70**, 115315 (2004).
[7] J. Voit, Rep. Progr. Phys. **58**, 977 (1995).
[8] D. Loss, Phys. Rev. Lett. **69**, 343 (1992).
[9] X.G. Wen, Phys. Rev. B **41**, 12838 (1990); A.M. Chang, L.N. Pfeiffer, and K.W. West, Phys. Rev. Lett. **77**, 2538 (1996).
[10] A. Yacoby *et al.*, Phys. Rev. Lett. **77**, 4612 (1996).
[11] J.U. Kim, J.M. Kinaret, M.-S. Choi, cond-mat/0403613.
[12] A. Braggio, *et al.*, Europhys. Lett. **50**, 236 (2000).
[13] A. Braggio, R. Fazio, and M. Sassetti, Phys. Rev. B **67**, 233308 (2003).
[14] O. Sauret, and D. Feinberg, Phys. Rev. Lett. **92**, 106601 (2004).
[15] A.B. Bortz, M.H. Kalos, and J.L. Lebowitz, J. Comput. Phys. **17**, 10 (1975).
[16] M.P. Schwarz, *et al.*, Phys. Rev. B 68, 245315 (2003).
[17] H.R. Shea, R. Martel, and Ph. Avouris, Phys. Rev. Lett. **84**, 4441 (2000).
[18] H.W. Schumacher, *et al.*, Appl. Phys. Lett. **75**, 1107 (1999).

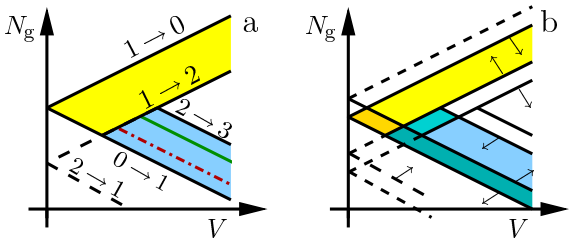

FIG. 1: Scheme of conducting regions in the $(V, N_{\rm g})$ plane. (a) $\Phi = 0$. Black lines: onset of the transitions $|J| \to |J'|$. Solid lines: detectable in current. Yellow: $J_{\max} = 1$; cyan: $J_{\max} = 2$. (b) $0 < \Phi < \Phi_0/2$. Each line of (a) is now split in two. Arrows indicate lines shift with increasing Φ.

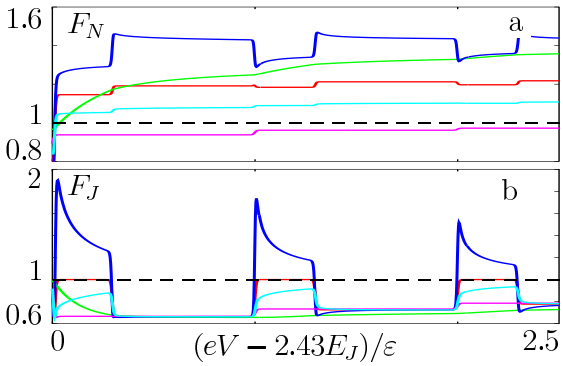

FIG. 2: Fano factors as a function of $(eV - 2.43E_J)/\varepsilon$, where V varies according to $N_g = 1/2 + 0.93E_J/E_N - eV/2E_N$, with $k_BT = 0.02E_J$ and $A = 20$. (a) F_N for an interacting ring, $g = 0.7$, and different interactions in the leads: $g_\ell = 1$ (red), 0.9 (cyan), 0.5 (green), 1.2 (blue); magenta: $g = g_\ell = 1$. (b) F_J, parameters and colors as in (a).

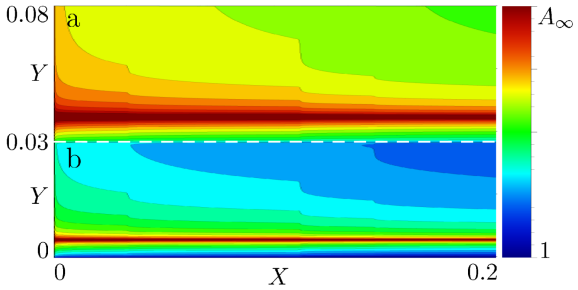

FIG. 3: Color-contour plot of A_c for $g = 0.7$, $g_\ell = 0.8$, $k_BT = 0.02E_J$ in the XY plane (see text). (a) Region I, $A_\infty = 4100$. (b) Region II, $A_\infty = 2.6\ 10^5$.

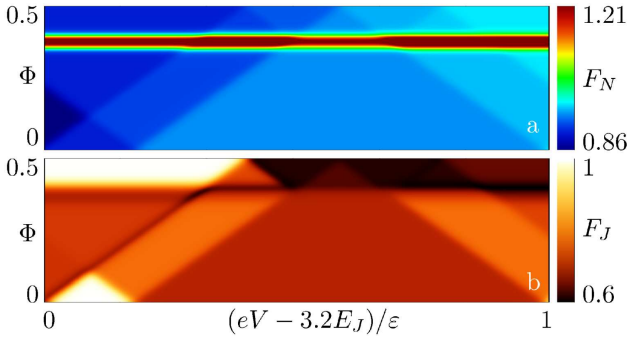

FIG. 4: Density plot of F_N (a) and F_J (b) as a function of $(eV - 3.2E_J)/\varepsilon$ (voltage moving according to $N_g = 1/2 + 1.7E_J/E_N - eV/2E_N$) and Φ, in units Φ_0. Parameters are: $g = 0.8$, $g_\ell = 1$, $k_BT = 0.02E_J$ and $A = 20$.

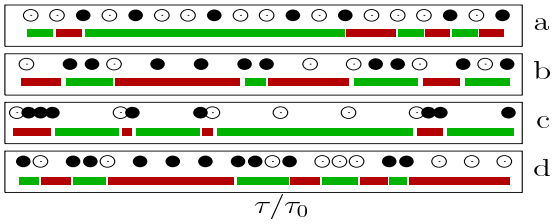

FIG. 5: Output sequences of a Monte-Carlo simulation for tunneling events at junction 2, with $eV = 3E_J$, $N_g = 0.48$, $k_BT = 0.02E_J$ and $A = 20$. Black (white) dots denote a clockwise (anticlockwise) entering electron. Colored bars are the sequence of the orbital value $|J|$, green: oscillations $0 \to \pm1 \to 0$; red: oscillations $\pm2 \to \pm1 \to \pm2$; (a) $g = g_\ell = 1$; (b) $g = 0.7$, $g_\ell = 1$; (c) $g = 0.7$, $g_\ell = 0.5$; (d) $g = 0.7$, $g_\ell = 1.2$.